Tools, Models and Dataset for IEEE 802.11ay CSI-based Sensing

Steve Blandino[1], Tanguy Ropitault[1,2], Anirudha Sahoo[1], Nada Golmie[1]
[1]Wireless Networks Division, National Institute of Standards and Technology, Gaithersburg, MD 20899 USA
[2]Prometheus Computing LLC, Sylva, NC, USA
steve.blandino@nist.gov

2022 IEEE Wireless Communications and Networking Conference (WCNC) | 978-1-6654-4266-4/22/$31.00 ©2022 IEEE | DOI: 10.1109/WCNC51071.2022.9771569

***Abstract*—The ubiquitous deployment and availability of wireless communications devices, coupled with recent technical advancements, provide a unique opportunity to enable wireless sensing applications, leveraging existing communications equipment and signals. The availability of modeling tools and dataset is crucial to support the development of sensing techniques and to understand the end-to-end performance of a joint wireless communication and sensing system. However, most of the sensing performance evaluations are carried out using proprietary tools and dataset. In this paper, we present a set of open source tools and models enabling the evaluation of future WLAN sensing systems. Our framework is composed of a ray-tracing implementation specific for sensing application, an IEEE 802.11ay physical layer (PHY) digital transceiver model and a visualization application. Using these tools, we design a dataset consisting of more than 14 000 entries of millimeter wave channels and IEEE 802.11 ay signals to democratize the design of both data-driven and model driven communication and sensing algorithms. We also provide a preliminary evaluation of a CSI-based WLAN sensing system using IEEE 802.11 ay signals. The results indicate that existing communication systems can be used to enable sensing applications.**

I. Introduction

Wireless channels can only provide finite resources for sensing and wireless data communication. These systems have been historically designed and used independently, thus competing against each other for spectrum usage. While spectrum sharing techniques are available [1], use cases for simultaneous sensing and wireless communication systems have gained a tremendous interest in the recent past. Although the current sensing radar systems can achieve a centimeter level resolution [2], and the wireless networks can support a multi-Gbps throughput [3], both wireless systems use the same spectrum and hence, act as interferer to each other, which negatively impacts their respective performance. To optimize the spectrum utilization, a joint communication and sensing system design should minimize the mutual interference, thereby improving the performance of both the systems.

Sensing through wireless communication networks aims at utilizing communication signals to detect and sense targets enabling application such as human presence detection, gesture recognition, or object tracking, while still providing communication. Remote monitoring can be achieved using the illumination offered by Wi-Fi signals. Hence, Wi-Fi devices can act as sensing nodes, using the principles of bistatic or multistatic radar [4]. The ubiquitous deployment and availability of wireless communication devices open the door to new sensing opportunities by leveraging existing communications equipment and signals. Thus, future generation of wireless communication systems are envisioned to support sensing capabilities. For instance, IEEE 802.11bf Task Group (TGbf) [5] is currently defining the appropriate amendments to existing Wi-Fi standards (IEEE 802.11 ad/ay/ax/ac/n) to enhance sensing capabilities through IEEE 802.11 devices.

The availability of modeling tools and dataset is crucial to support the development of sensing techniques and to understand the end-to-end performance of a joint wireless communication and sensing system. Currently, almost all sensing performance evaluations are carried out using proprietary dataset, obtained trough private measurements campaign [6]. Usually, system designer recruits participants to collect data, for instance, channel state information (CSI), received signal strength indicator (RSSI), or raw signals and the experiment is designed according to the requirements of the application. Thus, a comprehensive evaluation and comparison among different algorithms and design solutions is not straightforward. Only few dataset are currently publicly available. [7] and [8] provide radar received signal measurements at 5.8 GHz with 80 MHz bandwidth and at 77 GHz with 3.6 GHz bandwidth respectively. They provide a dataset of human actions such as walking, walking with hands in pockets, sitting down, standing up, picking an object, drinking and falling. [9], [10], [11] are based on an open dataset of wireless communication measurements at 60 GHz with 1.76 GHz bandwidth. The dataset consists of spatial beam signal to noise ratio (SNR), i.e., the SNR achieved with different beam combinations at the transmitter and the receiver, and RSSI in an indoor environment.

However, a dataset providing the raw received wireless communication signal and the full CSI with one or multiple active targets in the scenario is yet to be made available to the community. In this paper, we provide a sensing framework, publicly available on GitHub [12], composed by a ray-tracing implementation specific for sensing application, an IEEE 802.11ay PHY digital transceiver model and a visualization application. Using these tools, we design a dataset of millimeter wave (mmWave) channels and IEEE 802.11 ay received signals tailored to human sensing studies [13].

The main contributions of this paper can be summarized as follows:

1) We extend the quasi-deterministic (Q-D) channel methodology used in IEEE 802.11 ay, introducing the

notion of target. The contribution of the target(s) to the channel impulse response (CIR) is an additional cluster of rays that we obtain thanks to ray tracing techniques, as considered in the most recent TGbf contributions [14], [15], [16].

2) We share a public dataset, which consists of synthetically generated indoor mmWave channels between a multi-antenna transmitter and a multi-antenna receiver for various targets and channel configurations. The number of targets, velocity of each target and trajectory are randomized across the dataset. The dataset also contains received IEEE 802.11 ay signals.
3) We provide a performance evaluation of future WLAN sensing systems based on a IEEE 802.11ay waveform. Considering a CSI based sensing architecture, a SISO communication link is established between two nodes. The sensing processor estimates the CSI and computes the range-doppler map to detect motion.

The rest of the paper is organized as follows: Section II introduces a channel model for sensing systems based on ray tracing. Section III describes the signal model and the receiver signal processing. Section IV presents the open-source software and dataset design. Section V proposes a first evaluation of a future WLAN sensing system, based on a IEEE 802.11ay waveform. Section VI concludes the paper.

II. Channel Model for Joint Communication and Sensing

A. Preliminaries

The channel modeling effort performed at IEEE for mmWave Wi-Fi selected the Q-D methodology as the reference channel model [17]. The Q-D methodology is based on the observation that the wireless channel can be well described with a set of distinct geometry-based propagation paths [18]. This approach represents the millimeter-wave channel CIR by classifying a set of all CIR rays in a few deterministic strong rays (D-rays, originating from macro-objects reflections), and a number of relatively weak random rays (R-rays, originating from other static surfaces reflections). Dynamic objects are described through flashing rays (F-rays, originating by reflections from moving cars, buses and other dynamic objects) as stochastic processes which do not include any spatial or temporal constraints.

While this model has been successful in designing IEEE 802.11ad/ay algorithms, a wireless channel model for sensing applications should also provide consistency in both spatial and time domains to enable a realistic micro-doppler description, which is the most common signal processing technique for extrapolating dynamic information, such as speed and range of a moving target.

B. T-Rays Modeling

A new entity needs to be defined in a sensing channel model to enable the analysis of remote monitoring applications: the target, i.e., a dynamic object or person, moving with spatial and temporal consistency. Both large-scale and small-scale parameters of the channel need to vary with the position of the WLAN nodes, the targets, and the environment. Moreover, large-scale and small-scale parameters needs to be correlated over time when the WLAN nodes or targets move.

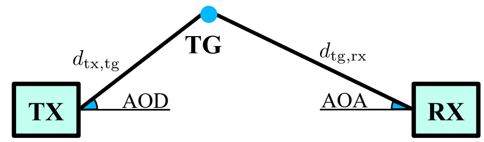

Fig. 1: T-rays modeling in a bi-static sensing system.

Motivated by these requirements, observed in experimental measurements [19], we introduce target related rays (T-rays), defined as relatively weak deterministic rays originated from dynamic targets *scattering*. Ray tracing, already used for the description of the reflections from macro-object [17], can also be an effective technique to provide a first order approximation of the interaction between the wireless signals and the targets. While both D-Rays and T-rays use ray tracing techniques, they represent two different electromagnetic phenomena. D-Rays describe strong reflections from macro-objects, also referred as specular components. On the contrary T-rays are defined as deterministic rays describing the backscattering signal. The backscattering signal includes a broader spectrum of electromagnetic phenomena beyond reflection, such as diffuse reflections and diffraction caused by irregular and finite targets.

Figure 1 shows a T-rays modeling for sensing applications in a bi-static configuration, i.e., the transmitter (Tx) and the receiver (Rx) are not co-located, but the proposed T-ray modeling is valid also for mono-static configurations, i.e., when Tx and Rx are co-located. Direct backscattering ray, i.e., the ray following the path originated at the Tx, impinging on a target and bouncing off the target, until reaching the Rx, is deterministically modeled to guarantee the spatial and temporal consistency required by sensing applications. The direct backscattering ray delay τ is computed from the model geometry:

$$\tau = \frac{d_{\mathrm{tx,tg}} + d_{\mathrm{tg,rx}}}{c}, \tag{1}$$

where $d_{\mathrm{tx,tg}}$ is the distance between the transmitter and the target, $d_{\mathrm{tg,rx}}$ is the distance between the target and the receiver and c is the speed of light. The distance $d_{\mathrm{tx,tg}} + d_{\mathrm{tg,rx}}$ is referred as the bi-static distance. The direct backscattering ray power is computed from the free space bi-static path loss β_{tg}, defined as:

$$\beta_{\mathrm{tg}} = \frac{\sigma_{\mathrm{tg}}(\mathbf{\Omega}_{\mathrm{tg}}^{\mathrm{AOA}}, \mathbf{\Omega}_{\mathrm{tg}}^{\mathrm{AOD}})\lambda_0^2}{(4\pi)^3 d_{\mathrm{tx,tg}}^2 d_{\mathrm{tg,rx}}^2}, \tag{2}$$

where λ_0 is the wavelength and $\sigma_{\mathrm{tg}}(\mathbf{\Omega}_{\mathrm{tg}}^{\mathrm{AOA}}, \mathbf{\Omega}_{\mathrm{tg}}^{\mathrm{AOD}})$ is the bi-static radar cross section (RCS), i.e., an attenuation coefficient, which depends on the vector $\mathbf{\Omega}_{\mathrm{tg}}^{\mathrm{AOA}}$, i.e., the Angle of Arrivals (AOAs) at the target in both azimuth and elevation and the vector $\mathbf{\Omega}_{\mathrm{tg}}^{\mathrm{AOD}}$, i.e., the Angle of Departures (AODs) from the target in both azimuth and elevation. AODs and AOAs can be easily computed using the geometry of the environment and the position of targets and WLAN nodes, for example, by applying the method of images [20].

In general, a complex target can be modeled as a group of individual N_T scattering centers distributed over the 3 dimensional space. Each scattering center contributes to the RCS of the complex target. Decomposing a complex target into multiple scattering centers is necessary especially in wideband applications, having a very high delay resolution. Since the target backscattered energy may span multiple delay (range) bins, for each delay bin, the average RCS represents the contributions from all scattering centers that fall within that bin [21].

C. Channel Model Including Human Targets: Boulic Model

Human sensing is considered in most of the IEEE 802.11bf use cases [22], hence it is of paramount importance to accurately model these applications. Human gait modeling has been an active research area in many fields such as biomedical engineering and sports medicine. A global human walking model based on an empirical mathematical models using biomechanical experimental data was proposed by Boulic et al. in [23]. The global walking model averages out the personification of walking and it has been successfully used in radar system design [24]. The Boulic model proposes a set of parameterized trajectories to represent both the position of the body in space and the internal body configuration and it is designed to keep the spatial and temporal correlation of an average human body. The model describes the motion of 17 joints (16 body segments) as shown in Figure 2a.

In the channel model presented in this paper, each joint is considered as a scattering center of the human target. Thus the human shape is simplified into a group of $N_T = 17$ individual target scattering centers. As shown in Figure 2b, each scattering center contributes to the channels response with a unique ray, which is accurately ray traced. The proposed ray tracing method also allows to analyze higher order multipath reflections, for instance, to include the target's projection on walls, ceiling and floor, as depicted in Figure 2b. This artifact caused by the multipath propagation, usually known as multiple ghosts, induces the sensing device to declare the presence of targets that do not physically exist in the actual scene.

Note that each of the scattering center might have a different scattering property, i.e. a different bi-static RCS. Thus, each joint can be described with a unique $\sigma_{\mathrm{tg}}(\mathbf{\Omega}_{\mathrm{tg}}^{\mathrm{AOA}}, \mathbf{\Omega}_{\mathrm{tg}}^{\mathrm{AOD}})$.

D. Communication and Sensing Channel Model

The double directional channel impulse response (DDIR) of a static (we do not consider F-rays in this work) environment with moving targets can be expressed as:

$$h(t, \tau, \mathbf{\Omega}^{\mathrm{AOD}}, \mathbf{\Omega}^{\mathrm{AOA}}) = h_{\mathrm{u}} + h_{\mathrm{r}}. \tag{3}$$

h_{u} refers to the target-unrelated channel, i.e., the channel relative to the environment, which can be modeled with the conventional IEEE 802.11 ay channel model described in Section II-A. h_{r} refers to the target-related channel, which can be modeled as a superposition of T-Rays in both space and time domain, formally as:

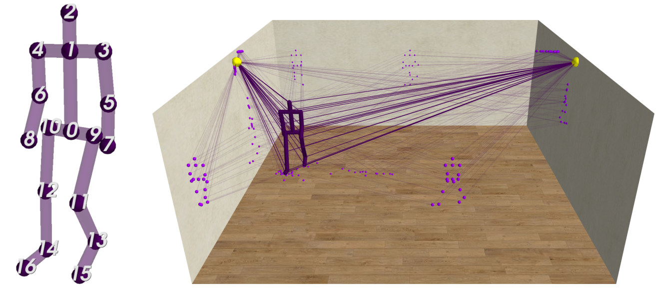

(a) Boulic Model (b) T-rays ray tracing including direct backscattering and ghosts reflections

Fig. 2: Channel model including human targets.

$$\begin{aligned} &h_{\mathrm{r}}(t, \tau, \mathbf{\Omega}^{\mathrm{AOD}}, \mathbf{\Omega}^{\mathrm{AOA}}) = \\ &\sum_{n=1}^{N_t} a_n(t, \sigma_{\mathrm{tg}}) \mathrm{e}^{-j2\pi f_n t} \delta(\tau - \tau_n(t)) \cdot \\ &\delta(\mathbf{\Omega}^{\mathrm{AOD}} - \mathbf{\Omega}_n^{\mathrm{AOD}}(t),\, \mathbf{\Omega}^{\mathrm{AOA}} - \mathbf{\Omega}_n^{\mathrm{AOA}}(t)), \end{aligned} \tag{4}$$

where a_n represents the complex amplitude of the n-th T-ray and implicitly depends on $\mathbf{\Omega}_{\mathrm{tg}}^{\mathrm{AOA}}$, and $\mathbf{\Omega}_{\mathrm{tg}}^{\mathrm{AOD}}$, since it is a function of σ_{tg}. τ_n and f_n are the delay and the Doppler shift, respectively. $\mathbf{\Omega}_n^{\mathrm{AOD}}$ and $\mathbf{\Omega}_n^{\mathrm{AOA}}$ are the AOD at the Tx and AOA at the Rx, respectively. The DDIR in Eq. (3) describes the propagation channel, without including the effect of the system. It can be converted into the system level CIR by applying antenna effects and band-limiting filters [17].

III. Wi-Fi Sensing System Model and Signal Processing

In this paper, we consider an IEEE 802.11ay single carrier (SC) system to enable sensing applications. We assume a SISO link composed of a transmitter and a receiver, in an indoor environment, which is generating a significant multipath effect and dense clutters, as shown in Figure 2. In the following, we consider a CSI based sensing WLAN scenario. The CSI, which is already available in a conventional IEEE 802.11ay system, is used to sense the environment by tracking the channel variations over time. Assuming static transmitter and receiver, a perturbation of the CSI is caused by a change in the environment, such as a moving target. We assume that the receiver is the initiator of the sensing session, i.e., it is the node requesting sensing information. Moreover, we assume that the receiver acts as the sensing processor, beyond a communication receiver. The transmitter sends IEEE 802.11ay packets continuously.

The EDMG SC frame is made of two main parts: the preamble and the data. The preamble contains known pilots sequence, namely Golay sequences, in the legacy short time field (L-STF), in the EDMG-STF, in the legacy channel estimation field (L-CEF) and in the EDMG-CEF.

STF and CEF are used in the communication receiver signal processing, for time and frequency synchronizations and channel estimation. These operations are achieved in multiple steps: i) First, the frame is detected and synchronized by finding the peak of the correlation between the received signal and the known STF pilots. ii) Then coarse frequency offset is computed by comparing the phase changes into the peaks of the STF correlation. iii) Finally, joint frequency offset and channel estimation is performed by correlating the received CEF with the known CEF.

From a remote sensing perspective, the channel estimated using the preamble can be seen as echoes from the targets and the environment. The delay of the echoes from the targets MPCs are proportional to the bi-static distance $d_{\mathrm{tx,tg}} + d_{\mathrm{tg,rx}}$, as shown in Eq. (1). As the IEEE 802.11ay packets are sent continuously over time, the sensing processor can build the radar data matrix, collecting the estimated CIR at each packet reception in a 2-dimensional matrix, i.e., the delay (referred also as fast time) and the evolution over the time (referred also as also slow time). To obtain the velocity of the targets, a discrete Fourier transform (DFT) is applied on the slow time dimension of the radar data matrix to allow the estimation of the target speed. Component with null velocity are considered static clutter, i.e., echoes coming from the static environments, thus they are not relevant to the remote monitoring. They can be filtered out, by removing the continuous component along the slow time dimension of the radar data matrix.

IV. Open Source Tools and Dataset

In this section, we review a set of open source tools that we have developed and publicly shared in [12], to support joint communication and sensing system design and evaluation. Using these tools, we have designed a dataset [13] of more than 14 000 channels and received IEEE 802.11 ay signals, which can be used to design both data-driven or model driven receiver algorithms.

A. NIST Q-D channel realization software

The NIST Q-D channel realization software provides a flexible, scalable and realistic channel model based on measurement campaigns to promote the design of new generation wireless communication and sensing systems at mmWave bands. The software is a full 3D ray tracing model that captures the geometrical properties of the channel between two reference points in space. The software generates a 3D multi-point to multi-point double directional CIR providing the magnitude, phase, time of arrival, AOD, and AOA of individual propagation paths between multiple points in space, thus supporting spatial correlation between different MIMO streams. The software has been enhanced to support the ray tracing of targets as explained in Section II.

B. NIST IEEE 802.11ay PHY

The NIST IEEE 802.11ay PHY [25] is a digital transceiver model including the main features of the IEEE 802.11ay PHY. It supports SU-MIMO and MU-MIMO for both OFDM and SC modes. It also supports several precoder and equalizer options, such as SVD, ZF precoder, block diagonalized-ZF precoder, and MMSE equalizer. The proposed digital transceiver can perform time synchronization of the received signal, frequency correction as well as estimating the channel using the preamble provided in the IEEE 802.11ay packet. The software has been enhanced to support the sensing signal processing presented in Section III, generating range-doppler maps from the estimated CSI.

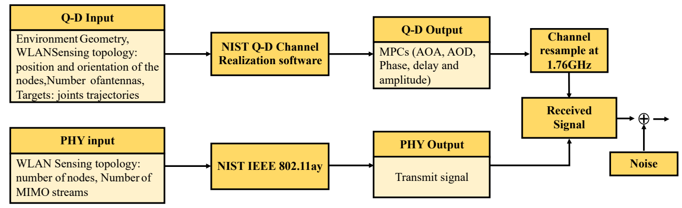

Fig. 3: Open source tools used to generate the dataset.

C. NIST Q-D Interpreter Software

The NIST Q-D Interpreter software has been developed to help visualizing the wireless signal propagation and investigate IEEE 802.11ad/802.11ay algorithms results using 3D visualization. This software uses input from both the NIST Q-D Channel Realization software and the NIST IEEE 802.11ay PHY. The software visualizes the interaction between the wireless signals and human moving targets, as shown for instance in Figure 2b and it displays range-Doppler maps time synchronized with the targets motion.

D. Dataset

Using the NIST Q-D channel realization software and the NIST IEEE 802.11ay PHY, we have generated a dataset consisting of more than 14 000 entries to engage the broad community to develop and test algorithms for communication and sensing in the 60 GHz band.

The process of generation of the dataset is illustrated in Figure 3. The geometry of the environment and the geometry of the WLAN scenario, e.g., position of the nodes and targets are defined in the NIST Q-D channel realization software. The target model is given as input to the Q-D software, which returns the MPCs as given in Eq. (4). The NIST IEEE 802.11ay PHY is configured with the number of MIMO streams and the MIMO precoding scheme (hadamard precoding) and it generates the IEEE 802.11ay waveform. To keep the size of the dataset limited, the transmit signal includes only the EDMG-CEF.

The dataset consists of synthetically generated indoor mmWave MIMO channels between a 4 antenna transmitter and a 4-antennas receiver. The room is of dimension $7\,\mathrm{m} \times 7\,\mathrm{m} \times 3\mathrm{m}$ and the WLAN devices are placed just below the ceiling level in the left and right walls as shown in Figure 2b.

Multiple human targets are moving in the room. We consider only direct backscattering signals coming from the targets, i.e., no ghosts are presents. The number of targets is randomized across the dataset. Each entry can have a random number of targets between 1 and 8. Also the velocity of each target and the trajectory are randomized across the dataset. The targets trajectories are generated with an acceptance-rejection

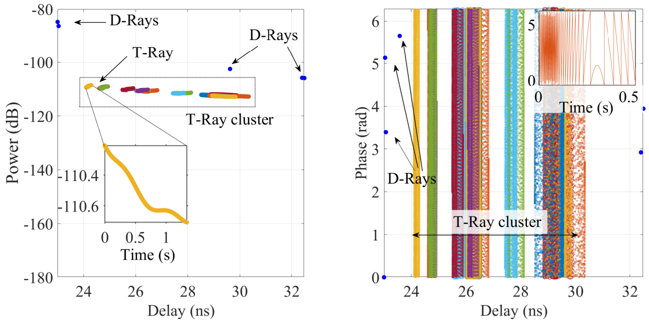

(a) Power Delay Profile (b) Phase vs Delay

Fig. 4: Time domain DDIR of a SISO WLAN sensing topology, including a moving human target.

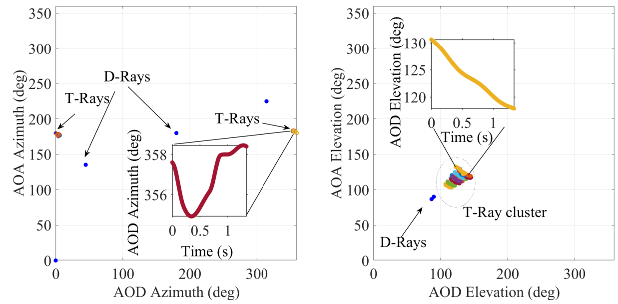

(a) Azimuth AOA vs AOD (b) Elevation AOA vs AOD

Fig. 5: Angular Domain DDIR of a SISO WLAN sensing topology including a moving human target.

method to avoid targets crossing each other. Each dataset point contains 128 channel realizations, with a sampling rate of 1 ms, thus describing a motion of 128 ms.

In the following, we analyze the main properties of a SISO bi-static channel with a single moving target. The RCS $\sigma_{\mathrm{tg}}(\mathbf{\Omega}_{\mathrm{tg}}^{\mathrm{AOA}}, \mathbf{\Omega}_{\mathrm{tg}}^{\mathrm{AOD}})$ is considered isotropic, i.e., each scatter center after being illuminated by RF energy radiates uniformly towards all the directions. Thus, σ_{tg} is constant over the angular dimensions. In the generation of the DDIR we consider only the deterministic rays, i.e., T-rays and D-rays.

1) Time Domain: Figure 4 shows a sequence of 128 consecutive channel impulse response realizations. Each channel realization is held on the figure, to show the temporal evolution (over the slow time) of the channel impulse response. Figure 4a shows the power delay profile of the channel impulse response. Since the WLAN nodes and the environment are assumed static, the power of the D-rays MPCs does not change over time. On the contrary, since the human target is moving, the T-rays, describing the target related channel, present a power variation over time. The T-rays cluster is composed of $N_T = 17$ different joints and each joint contributes differently over time, due to their different motion pattern. For example, the figure zooms into the dynamics of the first joint, showing a variation of 0.5 dB in a 1.34 s of simulated motion. Figure 4b shows instead the variation of the phase over time. As for the power description, the phase of the environment is static over time, hence D-rays do not present any phase fluctuation over time. The T-rays instead exhibit time-correlated phase fluctuation. The figure zooms into the last target MPC contribution that corresponds to the joint of the right foot. The phase variation shows the bio-mechanic of the gait cycle with a deceleration phase, a stance phase with very slow phase variation over time, and a final acceleration.

2) Angular Domain: The DDIR provides a discrimination of the different paths also in the spatial dimension, which can be used, for example, to design beamforming algorithms. Figure 5a and 5b show the evolution over the slow time of AOA vs AOD in azimuth and elevation, respectively. In the azimuth dimension the T-Rays are very close together and a small angular variation over time can be observed (see the inset in Figure 5a) in azimuth (3° fluctuation in AOD). As also shown in Figure 2b, in the considered configuration, the target provides a larger angular spread in the elevation plane. All the joints show a large fluctuation over time, for example, in the inset figure a variation of around 15° in AOD is observed.

V. Evaluation of CSI-based WLAN Sensing with IEEE 802.11ay signals

In this section we investigate the performance of an IEEE 802.11ay PHY as a sensing technology. We consider the scenario presented in Figure 2, consisting of two WLAN nodes and a single human target moving. The channel includes only deterministic components, i.e., D-Rays up to first order reflections and direct backscattering T-Rays. We consider a SISO EDMG SC transmission. The transmitter, includes scrambler, LDPC encoder, stream parser and constellation mapper. The receiver, after frame synchronization, frequency offset compensation and channel estimation, demodulates the SC symbols. Subsequently, the constellation demapping, stream deparsing and LPDC decoding are carried out to complete the PHY signal processing procedure. In the following we consider the modulation and coding scheme index 12, i.e., the SC blocks contain $\pi/2$ 16-QAM symbols with a coding rate of 1/2. The packet repetition frequency is 2 KHz and we assume a system bandwidth of 1.76 GHz. We assume an SNR of 30 dB. The sensing processor at the receiver collects N = 64 channel estimations to compute the radar data matrix. When the radar matrix is completed, the sensing processor performs a 64-length doppler FFT and converts the fast time bins into range bins. Figure 6 shows the simultaneous processing of the receiver WLAN node. The figure on the left shows the received 16 QAM constellation after the frequency domain channel equalization, with a measured EVM of −26 dB. On the right is the range-doppler map computed after the doppler FFT. The range-doppler map shows one stronger point, i.e., a major spike at around 1 m/s, which corresponds to the velocity of the target. The other points in the range-doppler map around the main spike are caused by the presence of other joints, which move at the walking speed of the target but they have also velocity and trajectory associated with the walking dynamics. By integrating the range-doppler map over

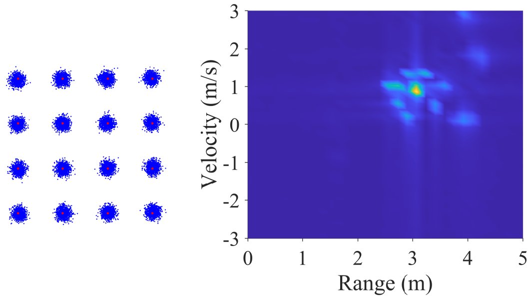

Fig. 6: Joint communication and sensing processing. A received 16-QAM constellation and range-Doppler map.

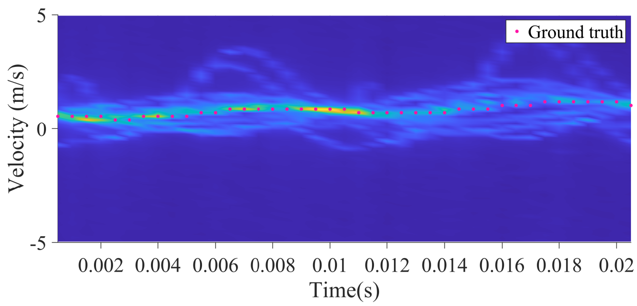

Fig. 7: Target velocity estimation over time using CSI.

the range domain, we present the analysis of the estimated velocity over time. Figure 7 shows the estimated velocity using the CSI. The figure shows that the target can be detected over time by using IEEE 802.11 ay signals. The stronger curve in the plot represents the walking speed of the target. The estimated values perfectly matches the true velocity, which is obtained assuming perfect CSI knowledge. The larger oscillations around the average speed indicate the presence of the other moving body parts.

VI. Conclusion

In this paper we have proposed a set of tools and models to design future joint communication and sensing systems. We have first presented an extension of the IEEE 802.11ay channel model introducing the notion of target. Thanks to the proposed models implemented in our open source framework, we designed a dataset of mmWave channels and IEEE 802.11ay received signals. The dataset, which is also shared publicly, can be used to investigate the performance of future communication systems as well as to design new data driven or model driven algorithms. Finally, we have provided a preliminary sensing performance evaluation using IEEE 802.11ay signals. Considering a CSI based sensing architecture, a SISO communication link is established between two nodes. The receiver measures the CSI and computes the range-doppler map to detect motion. The results indicate that existing communication system can be used to enable sensing applications. Joint communication and sensing systems are in their early stages and a significant amount of research still needs to be done to properly model and simulate their performance. For instance, the reflections properties of target objects needs to be accurately measured and modeled.

References

[1] R. Caromi and M. Souryal, "Detection of incumbent radar in the 3.5 GHz CBRS band using support vector machines," in *2019 Sensor Signal Processing for Defence Conference (SSPD)*, 2019, pp. 1–5.

[2] J. Lien, N. Gillian, M. E. Karagozler, P. Amihood, C. Schwesig, E. Olson, H. Raja, and I. Poupyrev, "Soli: Ubiquitous gesture sensing with millimeter wave radar," *ACM Trans. Graph.*, Jul. 2016.

[3] *Part 11: Wireless LAN (MAC) and (PHY) Specifications–Amendment 2: Enhanced Throughput for Operation in License-Exempt Bands Above 45 GHz*, IEEE Std. IEEE P802.11ay/D7.0, 2020.

[4] F. Colone, K. Woodbridge, H. Guo, D. Mason, and C. J. Baker, "Ambiguity function analysis of wireless LAN transmissions for passive radar," *IEEE Transactions on Aerospace and Electronic Systems*, vol. 47, no. 1, pp. 240–264, 2011.

[5] *802.11 SENS SG Proposed PAR Project Authorization Request (PAR)*, IEEE Std. IEEE 802.11-19-2103-11, 2021.

[6] L. Storrer, H. C. Yildirim, E. P. Copa, J. Louveaux, P. De Doncker, S. Pollin, and F. Horlin, "Experimental implementation of a multi-antenna 802.11ax-based passive bistatic radar for human target detection," in *2020 IEEE Radar Conference (RadarConf20)*, 2020, pp. 1–6.

[7] F. Fioranelli, S. A. Shah, H. Li, A. Shrestha, S. Yang, and J. Le Kernec, "Radar signatures of human activities," 2019.

[8] E. Gambi, G. Ciattaglia, A. De Santis, and L. Senigagliesi, "Millimeter wave radar data of people walking," *Data in Brief*, vol. 31, 2020.

[9] T. Koike-Akino, P. Wang, M. Pajovic, H. Sun, and P. V. Orlik, "Fingerprinting-based indoor localization with commercial MMWave WiFi: A deep learning approach," *IEEE Access*, vol. 8, 2020.

[10] M. Pajovic, P. Wang, T. Koike-Akino, H. Sun, and P. V. Orlik, "Fingerprinting-based indoor localization with commercial mmWave WiFi - part i: RSS and beam indices," in *2019 IEEE Global Communications Conference (GLOBECOM)*, 2019, pp. 1–6.

[11] P. Wang, M. Pajovic, T. Koike-Akino, H. Sun, and P. V. Orlik, "Fingerprinting-based indoor localization with commercial mmWave WiFi - part ii: Spatial beam SNRs," in *2019 IEEE Global Communications Conference (GLOBECOM)*, 2019, pp. 1–6.

[12] H. Assasa *et al.* (2021) A Collection of Open-source Tools to Simulate IEEE 802.11ad/ay WLAN Networks in Network Simulator ns-3. [Online]. Available: https://github.com/wigig-tools

[13] S. Blandino, R. Caromi, and T. Ropitault. Sensing using mmWave communications and ML. [Online]. Available: https://github.com/usnistgov/PS-002-WALDO

[14] M. Zhang *et al*, *Channel Models for WLAN Sensing Systems*, IEEE Std. IEEE 802.11-21-0782-02, 2021.

[15] T. Ropitault, S. Blandino, N. Varshney, and N. Golmie, *Q-D simulation and modeling framework for sensing*, IEEE Std. IEEE 802.11-21-0746-01, 2021.

[16] S. Blandino, T. Ropitault, N. Varshney, and N. Golmie, *A preliminary channel model using ray-tracing to detect human presence*, IEEE Std. IEEE 802.11-21-0747-01, 2021.

[17] *Channel Models for IEEE 802.11ay*, IEEE P802.11 Group for Wireless Local Area Networks (LANs) Std. IEEE 802.11-15/1150r9, 2015.

[18] A. Maltsev, A. Pudeyev, A. Lomayev, and I. Bolotin, "Channel modeling in the next generation mmWave Wi-Fi: IEEE 802.11ay standard," in *European Wireless 2016; 22th European Wireless Conference*, 2016.

[19] Y. Lv *et al.*, *Data-Driven Hybrid Channel Model for WLAN Sensing - 60GHz*, IEEE Std. IEEE 802.11-21-1365-00, 2021.

[20] A. Bodi *et al.* (2021) The NIST Q-D Channel Realization Software. [Online]. Available: https://github.com/wigig-tools/qd-realization

[21] B. R. Mahafza, *Radar systems analysis and design using MATLAB*. Chapman and Hall/CRC, 2005.

[22] A. Kasher, A. Eitan, S. Trainin, Y. Sun, and R. Du, *WiFi-Sensing-Use-Cases*, IEEE Std. IEEE 802.11-20-0611-16, 2020.

[23] R. Boulic, N. M. Thalmann, and D. Thalmann, "A global human walking model with real-time kinematic personification," *The visual computer*, vol. 6, no. 6, pp. 344–358, 1990.

[24] V. C. Chen, *The micro-Doppler effect in radar*. Artech House, 2019.

[25] J. Zhang, S. Blandino, N. Varshney, J. Wang, C. Gentile, and N. Golmie, "Multi-user MIMO enabled virtual reality in IEEE 802.11ay WLAN," in *2022 IEEE Wireless Communications and Networking Conference (WCNC)*, 2022, pp. 1–6.